A Combined QM/MM Method for the Determination of Regioselectivities in Rhodium-Catalyzed Hydroformylation

Dieter Gleich,† Rochus Schmid,‡ and Wolfgang A. Herrmann*,†

Anorganisch-chemisches Institut, Technische Universität München, Lichtenbergstrasse 4, D-85747 Garching, Germany, and Department of Chemistry, University of Calgary, 2500 University Drive, Northwest, Calgary, Alberta, Canada, T2N 1N4

Received June 3, 1998

Hydroformylation regioselectivities of rhodium−phosphine ligand systems are calculated according to a perspicuous formula that connects the regioselectivity of one phosphine coordination mode to the relative energies of the corresponding transition states of olefin insertion. If only one coordination mode is preferred—which may be fulfilled by bidentate chelating ligands—the formula quantifies the experimentally observed regioselectivities. To determine the relative transition-state energies, a combined QM/MM method with frozen reaction centers was applied and is discussed in detail. Tendencies in regioselectivites of four systems with the bidentate chelating ligands DIPHOS **4**, BISBI **5**, NAPHOS **6**, and the monodentate reference ligand triphenylphosphine (TPP) could be reproduced for the first time. As has been demonstrated previously, our method is also useful for the explanation of hydroformylation stereoselectivities.

Introduction

Hydroformylation is the largest-scale process of homogeneous organometallic catalysis with a capacity of over 6 million tons/year.[1] Butyric aldehyde, the hydroformylation product of propene, dominates over 70% of bulk chemical production with a ratio of linear to branched aldehyde (*n*:*iso*) near 95:5.[2] The regioselectivity $S_{n/iso}$ therefore plays an important role besides the general demand for high chemoselectivities. Additionally, *iso*-hydroformylation products of terminal or internal olefins exhibit a new chirality center (Chart 1). An enhanced stereoselectivity in hydroformylation would open new synthetic pathways to important fine chemicals.[3] Instead of former cobalt−carbonyl species, rhodium complexes modified by special ligands, usually phosphines, such as triphenylphosphine (TPP) or its water-soluble derivative TPPTS, are the predominantly used catalyst systems.[1] The fundamental catalytic steps, however, as proposed by Heck and Breslow[4] for cobalt, and by Wilkinson[5] for rhodium catalysts, are essentially identical (Scheme 1): olefin coordination (A); olefin insertion (B); CO insertion (C); oxidative addition of H_2 (D); reductive elimination of aldehyde (E). Kinetic investigations[1,6] suggest the rate-determining steps as D and E, respectively, whereas reaction B is fast and leads to *iso*- and *n*-alkyl complexes, which in turn give rise to the formation of linear and branched aldehydes. For that reason, olefin insertion is the crucial step for any qualitative and quantitative determination of regioselectivities. The preequilibria in Scheme 2 clearly demonstrate that $S_{n/iso}$ is subject to the partial pressure of CO and the ligand concentration. Two independent cycles and multiple phosphine coordination modes provide numerous active species, each with individual regioselectivities. Generally, cycle I should achieve better *n*:*iso* ratios, for the larger steric strain in 2-fold-coordinated phosphine complexes would raise the energetic spacing between *n*- and *iso*-insertion. This

Chart 1

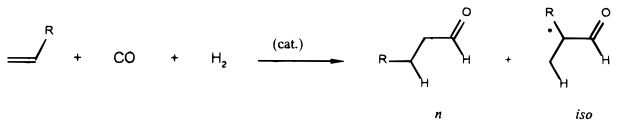

Chart 2

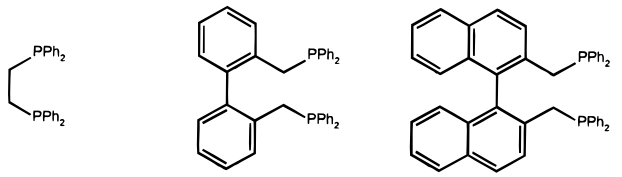

4 5 6

* To whom correspondence should be addressed. E-mail: lit@arthur.anorg.chemie.tu-muenchen.de.

† Technische Universität München.

‡ University of Calgary.

(1) Reviews: (a) Herrmann, W. A.; Cornils, B. *Angew. Chem., Int. Ed. Engl.* **1997**, *36*, 1047. (b) Cornils, B.; Herrmann, W. A. In *Applied Homogeneous Catalysis with Organometallic Compounds*; VCH-Wiley: Weinheim, 1996; Vol. 1, pp 3−25. (c) Cornils, B.; Herrmann, W. A.; Rasch, M. *Angew. Chem., Int. Ed. Engl.* **1994**, *33*, 2144.

(2) (a) Frohning, C. D.; Kohlpaintner, C. W. In *Applied Homogeneous Catalysis with Organometallic Compounds*; VCH-Wiley: Weinheim, 1996; Vol. 1, pp 29−104. (b) Herrmann, W. A.; Kohlpaintner, C. W. *Angew. Chem., Int. Ed. Engl.* **1993**, *32*, 1524.

(3) Botteghi, C.; Paganelli, S.; Schionato, A.; Marchetti, M. *Chirality* **1991**, *3*, 355.

(4) Heck, R. F.; Breslow, D. S. *J. Am. Chem. Soc.* **1961**, *83*, 4023.

(5) Evans, D.; Osborn, J. A.; Wilkinson, G. *J. Chem. Soc. (A)* **1968**, 3133.

(6) Tolman, C. A.; Faller, J. W. *New Syntheses with Carbon Monoxide*; Pignolet, L. H., Ed.; Springer: New York, 1983.

10.1021/om980459q CCC: $15.00
Publication on Web 10/08/1998

Scheme 1. Catalytic Cycle of Hydroformylation ($\langle M\rangle$−H = Active Species)

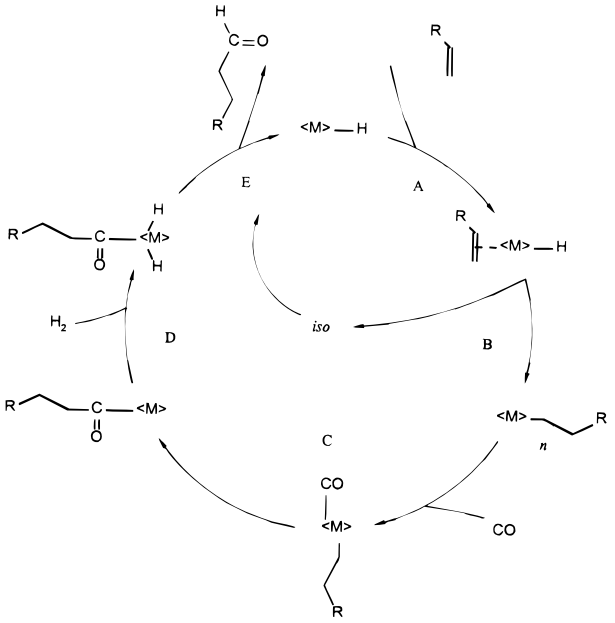

Scheme 2. Preequilibria of Two Catalytic Cycles with Different Active Species

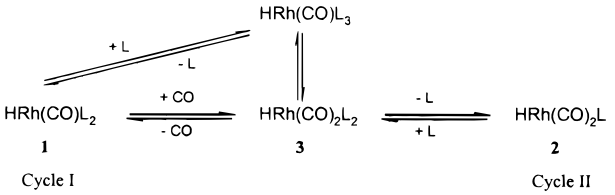

qualitative view reflects the actual situation disclosed at the beginning of a recent publication:[7] "While extensive screening of a wide variety of phosphine and phosphite ligands has been reported, no detailed understanding of how phosphines control regiochemistry has emerged." Nevertheless, owing to the impetuous progress in computational chemistry, a theoretical and more quantitative treatment seems to be feasible.

Preferences in phosphine coordination modes depend on the interplay of steric and electronic properties, whose most familiar description is found in Tolman's cone angle concept and correlation of IR frequencies.[8] Brown and co-workers have shown by NMR studies that in trigonal bipyramidal TPP−rhodium complexes of type **3** the phosphine axial:equatorial ratio is 85:15.[9] Coordination modes of bidentate chelating phosphines can be studied theoretically by molecular mechanics (MM) calculations such as Casey's natural bite angle (NBA) method.[10] Some correlations between bite angles and regio-
selectivities have been postulated.[10,11] Olefin insertion has been described by quantum mechanical (QM) methods.[12−15] Ziegler and co-workers studied the whole hydroformylation cycle of unmodified cobalt−carbonyl species with DFT calculations.[14] Morokuma and coworkers applied ab initio calculations (HF and MP2 level) on modified rhodium complexes.[15] They confined their calculations to cycle II in Scheme 2 and employed model systems with phosphine PH_3 and substrate ethylene. Although model systems are important for the study of elementary reaction steps, care must be taken when results are extrapolated to a more realistic case. It has been shown that PH_3 models neither the steric nor electronic characteristics of TPP.[16,17] MM methods, on the other hand, may handle "real" ligands or complexes, but can describe only steric effects explicitly. Beyond that, reaction paths with changes in atom connectivity (which is true for olefin insertion) cannot be calculated with MM methods because of fixed connectivities.[18] To tackle all these problems, an appropriate combination of QM and MM methods must be found.[16b,19]

If one assumes an irreversible olefin insertion and no changes in the *n*:*iso* distribution after the insertion step—two conclusions suggested by experiment[1,7]—it is straightforward to set up a formula that connects the regioselectivity of one coordination mode (Scheme 2) to the relative energies of the transition states.[20] Bidentate chelating ligands should prefer cycle I for entropic reasons. If the ligand fits well into geometric requirements, only one coordination mode may be preferred. The formula given above would then quantify the experimentally observed regioselectivities. In the following sections, we determine the regioselectivities of rhodium−phosphine ligand systems according to formula 1. To this end, we performed density functional

$$S_{n/iso} = \frac{R_n}{R_{iso}} = \frac{\sum_y k_{n,y}[\mathrm{E}]}{\sum_x k_{iso,x}[\mathrm{E}]} = \frac{\sum_y k_{n,y}}{\sum_x k_{iso,x}} = \frac{\sum_y \mathrm{e}^{-\Delta G^{\#}_{n,y}/RT}}{\sum_x \mathrm{e}^{-\Delta G^{\#}_{iso,x}/RT}} \cong \frac{\sum_y \mathrm{e}^{-E^{\#}_{n,y}/RT}}{\sum_x \mathrm{e}^{-E^{\#}_{iso,x}/RT}} \quad (1)$$

S = kinetic selectivity

R = reaction rate

k = rate constant

[E] = concentration of olefin complex

$G^{\#}$ = free energy of transition state

$E^{\#}$ = internal energy of transition state (arbitrary reference point)

theory (DFT) calculations on model rhodium complexes.[16] Based on these model system transition states,

(7) Casey, C. P.; Petrovich, L. M. *J. Am. Chem. Soc.* **1995**, *117*, 6007.
(8) Tolman, C. A. *Chem. Rev.* **1977**, *77*, 313.
(9) Brown, J. M. Kent, A. G. *J. Chem. Soc., Perkin Trans. 2* **1987**, 1597.
(10) Casey, C. P.; Whiteker, G. T. *Isr. J. Chem.* **1990**, *30*, 299.
(11) Casey, C. P.; Whiteker, G. T.; Melville, M. G.; Petrovich, L. M.; Gavney, J. A.; Powell, D. R. *J. Am. Chem. Soc.* **1992**, *114*, 5535.
(12) Thorn, D. L.; Hoffmann, R. *J. Am. Chem. Soc.* **1978**, *100*, 2079.
(13) Siegbahn, P. E. M. *J. Am. Chem. Soc.* **1993**, *115*, 5803.
(14) Versluis, L.; Ziegler, T.; Fan, L. *Inorg. Chem.* **1990**, *29*, 4530 and references therein.
(15) (a) Matsubara, T.; Koga, N.; Ding, Y.; Musaev, D. G.; Morokuma, K. *Organometallics* **1997**, *16*, 1065. (b) Koga, N.; Morokuma, K. *Chem. Rev.* **1991**, *91*, 823. (c) Koga, N.; Jin, S. Q.; Morokuma, K. *J. Am. Chem. Soc.* **1988**, *110*, 3417.

Table 1. Geometric and Energetic Parameters of the Model Systems

system	Rh−C_1 (Å)	Rh−H (Å)	C_1−C_2 (Å)	C_2−H (Å)	Rh−C_1−C_2 (deg)	H−Rh−C_1−C_2 (deg)	E (kcal·mol^{-1})
MSOI 1/ethene[a]	2.01	1.59	1.44	1.51	74.4	+10.3	+15.8
MSOI 1/propene/*iso*[b]	2.01	1.60	1.44	1.48	74.2	−12.1	0
MSOI 1/propene/*n*[b]	2.00	1.61	1.45	1.43	76.2	+15.0	1.4
MSOI 2/ethene[a]	2.19	1.64	1.41	1.71	74.4	−16.8	−5.2
MSOI 2/propene/*iso*[b]	2.22	1.64	1.41	1.73	73.4	+4.5	1.2
MSOI 2/propene/*n*[b]	2.19	1.64	1.41	1.69	75.3	+12.2	0

[a] Parameters for the total insertion process. [b] Parameters for the energetically favored transition states (see text).

Table 2. Force Field Parameters for All MM Calculations[a]

bond	potential	natural value (Å)	force constants (kcal·mol^{-1}·Å^{-2})	comment
Rh−C_1	harmonic	2.20	1000	fixed
Rh−H	harmonic	1.65	1000	fixed
C_2−H	harmonic	1.73	1000	fixed
Rh−P	harmonic	2.30	1000	fixed
Rh−CO	harmonic	1.90	1000	fixed

angle	potential	natural value (deg)	force constants (kcal·mol^{-1}·deg^{-2})	comment
Rh−C_1−C_2 (ϵ_1)	harmonic	76	1000	fixed
L_1−Rh−$L_{2,3}$ ($\alpha_{2,3}$)	harmonic	90	30	soft
$L_{2,3}$−Rh−C_1 ($\beta_{2,3}$)	harmonic	120	30	soft
L_2−Rh−L_3 (β_1)	harmonic	120	30	soft
L_1−Rh−H (γ_1)	harmonic	180	30	soft

torsion	potential	natural value (deg)	force constants	comment
Rh−C_1−C_2−H (δ_1)	torsion_3[b]	0	0	free

van der Waals	potential	natural value	force constants	comment
Rh	9,6[b]	r_0 = 2.00 Å ϵ = 0.20		estimated

[a] Cf. Scheme 3. [b] Cf. ref 30b.

force field calculations were carried out in order to incorporate steric effects. This combined QM/MM method with separate QM and MM calculations is related to approaches recently discussed in the literature.[19a,c] Systems with four different ligands have been studied: The bidentate chelates DIPHOS **4** and BISBI[21] **5** are ideally suited for a new theoretical treatment because (i) deuterioformylation experiments of Casey and co-workers have confirmed the irreversibility of olefin insertion[7] and (ii) the same authors made MM calculations with purely hypothetical transition-state geometries which could not reproduce the experimental observations. It is therefore possible (i) to start with experimentally supported assumptions and (ii) to test if our method is superior to the previous one. Further ligands are NAPHOS[22] **6**, a bidentate chelate which is built up analogously to BISBI **5**, and TPP, which serves as a monodentate reference ligand.

Computational Details

a. DFT Calculations. For all calculations, the DZVP basis set[23] was chosen. Further details about this basis set have already been discussed elsewhere.[16a] All structures were optimized without any restrictions on the LDA level of theory using the eigenvector-following technique.[24] The resulting geometries were verified to be first-order transition states by analytical calculation of the second energy derivative matrix. Total energies have been calculated with reasonable accuracy by a perturbative inclusion of gradient corrections[25] using the LDA geometry and density. The calculations were performed with the program DGauss[26,27a] and the UniChem Interface.[27b]

b. MM Calculations. All MM calculations were made with the cff91 force field[28] extended by phosphorus parameters.[22] Additional modifications are discussed below. To describe the complex geometries, a trigonal-bipyramidal metal coordination was assumed for all ligand-coordinated systems and realized by restraints implemented in the force field (cf. Table 2). Weak force constants were chosen in order to avoid rigid idealized geometries.[29] Atomic charges other than those of aryl rings were neglected. Suitable initial structures were subject to a 100 ps gas-phase MD simulation at constant high temperature (1000 K), a sampling technique that seems to be sufficient for this type of systems. Every picosecond the

(16) (a) Schmid, R.; Herrmann, W. A.; Frenking, G. *Organometallics* **1997**, *16*, 701. (b) Schmid, R. Ph.D. Thesis, Technische Universität München, Germany, 1997.
(17) González-Blanco, O.; Branchadell, V. *Organometallics* **1997**, *16*, 5556.
(18) Burkert, U.; Allinger, N. L. *Molecular Mechanics*; ACS Monograph 177; American Chemical Society: Washington, DC, 1982.
(19) (a) Nozaki, K.; Sato, N.; Tonomura, Y.; Yasutomi, M.; Takaya, H.; Hiyama, T.; Matsubara, T.; Koga, N. *J. Am. Chem. Soc.* **1997**, *119*, 12779. (b) Maseras, F.; Morokuma, K. *J. Comput. Chem.* **1995**, *16*, 1170. (c) Kuribayashi, H. K.; Koga, N.; Morokuma K. *J. Am. Chem. Soc.* **1992**, *114*, 8687.
(20) (a) Consiglio, G.; Pino, P. *Top. Curr. Chem.* **1982**, *105*, 77. (b) Glasstone, S.; Laidler, K. J.; Eyring, H. *The Theory of Rate Processes*; McGraw-Hill: New York, 1941.
(21) Herrmann, W. A.; Kohlpaintner, C. W.; Herdtweck, E.; Kiprof, P. *Inorg. Chem.* **1991**, *30*, 4271.
(22) Herrmann, W. A.; Schmid, R.; Kohlpaintner, C. W.; Priermeier, T. *Organometallics* **1995**, *14*, 1961.
(23) Godbout, N.; Salahub, D. R.; Andzelm, J.; Wimmer, E. *Can. J. Chem.* **1992**, *70*, 560.
(24) Baker, J. *J. Comput. Chem.* **1986**, *7*, 385.
(25) (a) Becke, A. *Phys. Rev. A* **1988**, *38*, 3098. (b) Perdew, J. P. *Phys. Rev. B* **1986**, *33*, 8822.
(26) Andzelm, J.; Wimmer, E. *J. Chem. Phys.* **1992**, *96*, 1280.
(27) (a) *DGauss 3.0*; Cray Research Inc., 1995. (b) *UniChem 2.3.1*; Cray Research Inc., 1994.
(28) Maple, J. R.; Dinur, U.; Hagler, A. T. *Proc. Natl. Acad. Sci. U.S.A.* **1988**, 5350.
(29) "Soft" restraints are equal to estimated force constants, whereas "hard" restraints fix a certain geometry.

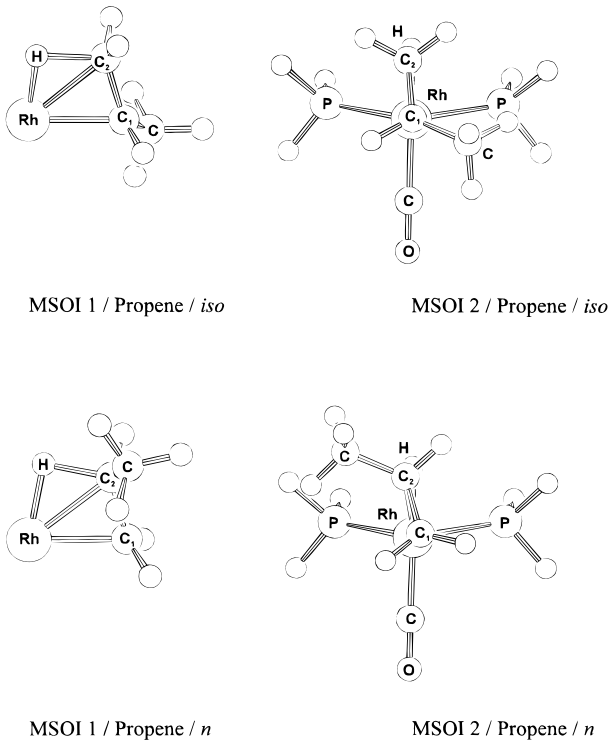

Figure 1. Model system transition states.

structures were minimized, and those with lowest energy were taken as global minima. The relative energies of the global minima were then used for regioselectivity calculations following formula 1. The temperature was chosen to be 298 K, although changes in temperature have only a small influence. The calculations were performed with the Insight/Discover program package.[30]

Results and Discussion

We will first treat the model systems for the MM calculations, then discuss several aspects of the combined QM/MM method, and finally compare our theoretical approach with experimental values and previous calculations.

a. Model Systems. The simplest model systems for olefin insertion (MSOI) solely consist of a naked metal−hydrido olefin unit.[13] The olefins chosen in our calculations are ethylene and propene (MSOI 1). In a further step, ligands (PH_3, CO) were added around the reaction center (MSOI 2). The DFT calculations with MSOI 2 are related to Morokuma's ab initio (HF and MP2) results,[15] but focus on complexes with two equatorially−equatorially coordinated phosphine ligands (cf. cycle I in Scheme 2).

Energetic and geometric comparison of corresponding reaction profiles (Table 1 and Figure 1) reveals three aspects:

(i) The insertion is endothermic for MSOI 1 and exothermic for MSOI 2. The energetic differences between *iso*- and *n*-insertion of propene, i.e., the regioselectivities, are also reversed. It is obvious that ligand coordination changes the energetic order drastically.

(ii) In the case of MSOI 1, propene insertion runs through two *iso*- and *n*-transition states, respectively,

(30) (a) *Insight/Discover, Release 95.0*; BIOSYM/MSI: San Diego, 1995. (b) *Discover 95.0/3.0.0 User Guide*; BIOSYM/MSI: San Diego, 1995.

Scheme 3. Reaction Centers (dashed lines) and Coordination Modes

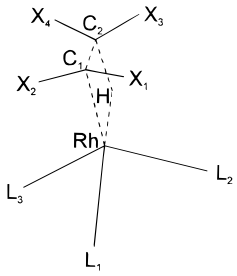

ee: $L_1 = CO$, $L_2 = L_3 = PR_3$

ae-1: $L_1 = L_2 = PR_3$, $L_3 = CO$

ae-2: $L_1 = L_3 = PR_3$, $L_2 = CO$

because both the methyl group and the H atom may occupy two sites of the Rh−C_1−C_2 plane. Only the energetically favored transition states (with opposite orientation of the methyl group and the H atom) are depicted in Figure 1. In the case of MSOI 2, these possibilities are doubled by different Rh−P distances. Again, only the transition states with lowest energies are shown.

(iii) For *iso*- and *n*-propene transition states, the geometries of the reaction centers, i.e., the four-membered cycles of olefin insertion without olefin substituents, are quite identical. The geometries of propene and ethylene reaction centers are also closely related. Moreover, in contrast to the energies, the geometries persist rather well when ligands have been added. Another similarity between MSOI 1 and MSOI 2 is that all transition states are of early nature. Corresponding Rh−C_1 and C_2−H distances, however, indicate that for MSOI 2 the transition states lie still closer to the starting olefin complex than for MSOI 1. Since the insertion occurs early especially for coordinated systems, the transition-state geometries of the entire complex are then still approximately trigonal bipyramidal.[31] Therefore, the contribution of solvent effects should be nearly the same for olefin complexes and transition states, and the use of gas-phase energies seems to be a reasonable approximation. Furthermore, the confinement to internal energies in formula 1 is justified by the similarities of all transition states.

b. MM Calculations with Frozen Reaction Centers. The geometry of the reaction centers was taken from DFT calculations (Table 2 and Scheme 3). In contrast to the DFT results, propene insertion for MSOI 1 runs through only one *iso*- and *n*-transition state, respectively. Moreover, the methyl group as well as the H atom occupies the same site of the Rh−C_1−C_2 plane. These distinctions stem from intrinsic force field properties: MM treatment raises the complex symmetry; electronic subtleties are neglected. As the Rh−P distance is fixed (Table 2), addition of ligands generally allows four transition states (Table 3 and Scheme 3). Analogous to MSOI 2, only the equatorial−equatorial (ee) arrangement of TPP was taken. BISBI **5** and NAPHOS **6** possess one chiral axis (point group C_2), while DIPHOS **4** is achiral. The bite angles of BISBI **5** and NAPHOS **6** (about 120°)[10] and DIPHOS **4** (about

(31) In ref 15, square pyramidal transition-state geometries of complexes with only *one* coordinated phosphine have been reported. However, the line between "approximately trigonal bipyramidal" and "square pyramidal" generally is not sharp, and the transition-state geometries of complexes with *two* equatorially coordinated phosphines are indeed rather trigonal bipyramidal (cf. Figure 1).

Table 3. Labeling of Propene Reaction Centers and Olefin Substituents X[a]

methyl group orientation[a]	TS[b]	angles, dihedrals[a]	name/parameters
$H_3C = X_1$	*iso-1*	$Rh-C_1-C_2$	ϵ_1/cf. Table 2
$H_3C = X_2$	*iso-2*	$Rh-C_1-X_{1,2}$	$\varphi_{1,2}$/cf. Table 4
$H_3C = X_3$	*n-1*	$H-C_2-X_{1,2}$	$\varphi_{3,4}$/cf. Table 4
$H_3C = X_4$	*n-2*	$Rh-C_1-C_2-H$	δ_1/cf. Table 2

[a] Cf. Scheme 3. [b] Transition state (see text).

Table 4. Force Field Parameters for Versions A and B[a]

version	bond	potential	natural value (Å)	force constants (kcal·mol^{-1}·Å^{-2})
A	C_1-C_2	quartic_bond[b]	1.41	same as for c=[b]
B	C_1-C_2	quartic_bond[b]	1.41	same as for c[b]

version	angle	potential	natural value (deg)	force constants (kcal·mol^{-1}·deg^{-2})
A/B	$\varphi_{1,2}$ (X = H)	harmonic	100	35
A/B	$\varphi_{1,2}$ (X = CH_3)	harmonic	100	40
A/B	$\varphi_{3,4}$ (X = H)	harmonic	100	40
A/B	$\varphi_{3,4}$ (X = CH_3)	harmonic	100	40

[a] Cf. Scheme 3. [b] Cf. ref 30b.

90°)[10] recommend an equatorial−equatorial and axial−equatorial (ae) arrangement, respectively. Thus, for both BISBI **5**/NAPHOS **6** and DIPHOS **4**, all four transition states in Scheme 3 are split up in energy ($x = y = 2$ in formula 1).[32] Since the MM potential energy surfaces of *iso*- and *n*-transition states are different, the energies have to be corrected (formula 2). A major

$$E'_{\mathrm{iso}} = E_{\mathrm{iso}} - E^0(\mathrm{MS}_{iso}) = E(\mathrm{L}) + E(\mathrm{NI}_{iso}) \qquad (2)$$

$$E'_n = E_{\mathrm{n}} - E^0(\mathrm{MS}_n) = E(\mathrm{L}) + E(\mathrm{NI}_n)$$

E^0(MS) = MM energy of isolated MSOI 1

E(L) = MM energy of ligands (PR_3, CO)

E(NI) = MM energy of nonbonding interactions between MSOI 1 and ligands

problem is that no experimental basis exists for a complete parametrization of the transition states. In particular, three uncertainties must be clarified: (i) parametrization of the carbon atoms $C_{1,2}$ and angles $\varphi_1-\varphi_4$, respectively; (ii) comparison of regioselectivities without restraints; and (iii) contribution of steric and electronic effects to the energetic differences of *iso*- and *n*-transition states.

b.1. Variable Parametrization of $C_{1,2}$ and $\varphi_1-\varphi_4$. To estimate how far the regioselectivities depend on C and φ parametrization, we performed MM calculations with different force field versions A−E (Tables 4 and 5): A, carbon atoms with sp^2 hybridization; B, carbon atoms with sp^3 hybridization; C, fixed force constants of φ angles (1000 kcal·mol^{-1}·deg^{-2}); D, natural values of φ angles lowered to 95°; E, natural values of φ angles raised to 105°.

As can be seen in Table 5, the φ dependence of ligand regioselectivities is strong, whereas C parametrization has a minor influence. The order of ligand regioselectivities, however, does not change: $S_{\mathrm{NAPHOS}} \geq S_{\mathrm{BISBI}} \gg S_{\mathrm{TPP}} \approx S_{\mathrm{DIPHOS}}$ for all versions. Therefore, one can conclude that φ parametrization affects mainly *absolute* selectivities.

(32) In our calculations, the (*R*)-enantiomers of **5**/**6** and arrangement ae-1 of **4** (cf. Scheme 3) were taken.

Table 5. Ligand Regioselectivities $S_{n/iso}$ of Force Field Versions A−G (Substrate = Propene)

ligand	$S_{n/iso}$ (A)	$S_{n/iso}$ (B)	$S_{n/iso}$ (C)	$S_{n/iso}$ (D)	$S_{n/iso}$ (E)	$S_{n/iso}$ (F)	$S_{n/iso}$ (G)
BISBI[a]	8.0:1	10.0:1	18.1:1	11.1:1	5.6:1	10.3:1	5.9:1
NAPHOS[a]	9.0:1	11.0:1	18.1:1	12.3:1	6.3:1	10.3:1	6.3:1
DIPHOS[b]	3.4:1	1.6:1	6.8:1	4.7:1	2.4:1	2.4:1	1.5:1
TPP[a]	3.5:1	3.2:1	5.5:1	3.7:1	3.2:1	3.4:1	2.0:1

[a] Selectivity for the equatorial−equatorial coordination mode. [b] Selectivity for the axial−equatorial coordination mode.

Table 6. DFT and MM Calculations of the Relative Transition-State Energies for Two Equatorially Coordinated Phosphine Ligands (Substrate = Propene)

$E^{\#}$ (kcal·mol^{-1})[a]	DFT[b]	MM[b,c]
iso, PH_3	1.2	0.1
n, PH_3	0	0
iso, TPP	−	0.7
n, TPP	−	0

[a] Relative energies of the energetically favored transition states (see text). [b] See Computational Details. [c] Force field version A (see text).

b.2. Variation of Restraints. Two further force field calculations are listed in Table 5: F, single-point energies of version A geometries without α, β, γ restraints (cf. Table 2 and Scheme 3); G, single-point energies of version A geometries without α, β, γ, and φ restraints (cf. Table 4 and Scheme 3).

Once more, no changes occur in the selectivity order. The purely steric energy contributions increase from A over F to G, while the electronic contributions (which have to be imposed on the MM systems) decrease successively. It is indispensable to optimize the MM structures with α, β, γ and φ restraints because otherwise unreasonable geometries will be obtained. It is, however, usual to subtract the share of "hard" restraints from the total energy.[18,29] Nevertheless, we have decided to choose version A for optimizations as well as energy calculations since the restraints are only "soft"[29] and the absolute selectivity values seem to be a compromise between the extremes of versions C and G (cf. Table 5).

b.3. Steric and Electronic Effects. It has been noted in the Introduction that only steric effects can be described explicitly by MM methods. The smaller the electronic contribution to the total energy is, the more reliable are the MM results. Results of DFT and MM calculations (substrate = propene) with PH_3 and PH_3/TPP, respectively, are shown in Table 6. For PH_3, the MM results have the same tendency as the DFT results, but the differences are negligibly small; electronic effects are dominant. Yet for TPP, the energetic spacing between *iso*- and *n*-transition states is shifted toward higher values; steric contributions are dominant. A similar behavior is expected also for the chelates DIPHOS **4**, BISBI **5**, and NAPHOS **6** (type alkyl−PPh_2). The question now arises if our method is able to describe the fundamental difference in regioselectivities between aliphatic olefins (e.g., propene) and conjugated olefins such as styrene. It is generally known that styrene is

Table 7. BISBI Regioselectivities $S_{n/iso}$ of Propene and Styrene

substrate	$S_{n/iso}$[a]
propene	8.0:1
styrene	15.6:1

[a] Force field version A (see text).

Table 8. Experimental versus Calculated Regioselectivities (Substrate = Propene)

ligand	$S_{n/iso}$ (exptl)[a]	$S_{n/iso}$ (calc)[b]	$S_{n/iso}$ (calc)[c]
BISBI	17.0:1	8.0:1[d]	24.8:1[d]
NAPHOS		9.0:1[d]	
DIPHOS	2.1:1	3.4:1[e]	34.8:1[e]
TPP	3.5:1	3.5:1[d]	

[a] Kinetic regioselectivities for the hydroformylation of hexene (cf. ref 7). [b] Force field version A (see text). [c] Energy values of ref 7, selectivity calculated with four transition states (cf. ref 34). [d] Selectivity for the equatorial−equatorial coordination mode. [e] Selectivity for the axial−equatorial coordination mode.

mainly converted to *iso*-aldehydes, whereas *n*-butyraldehyde dominates in the case of propene.[1,3] Model calculations (MSOI 1, substrate = butadiene) do not indicate that the *geometries* of the transition states are substantially different from those of aliphatic olefins, although allylic coordination may play an important role before and after the transition states.[16b] Based on these results, for our MM calculations the geometry of the reaction center has remained unchanged. Table 7 shows the results for BISBI **5** with propene and styrene, respectively. The regioselectivities are not opposite; on the contrary, they are higher for styrene than for propene. Therefore, we conclude that, in contrast to aliphatic olefins, electronic effects are prevailing for the transition-state *energies*. The electronic influence of the phenyl group is crucial for the energetic spacing between *iso*- and *n*-transition states, whereas the electronic influence of the methyl group (and presumably any other alkyl group) differs not extremely from that of a hydrogen atom; that is, electronic substrate contributions of *iso*- and *n*-transition states, respectively, are nearly the same. On the other hand, electronic substrate contributions of *iso*- or *n*-transition states should be nearly the same for aliphatic *and* conjugated olefins because the connectivities are identical. That is why the stereoselectivites (which are determined only via *iso*-transition states) can be calculated directly by our method, as has been demonstrated previously.[33]

c. Comparison with Experimental Values and Previous Calculations. We are now ready to compare our final results with previous ones. A summary is given in Table 8; transition states are shown in Figures 2 and 3. The olefin used in the experiment is hexene instead of propene, but there is no evidence for a significant change in regioselectivitiy.[1] Whereas Casey's approach[7] reverses the experimental tendencies, our approach gives the right order for DIPHOS **4** and BISBI **5**.[34] We are disposed to see the major reason for this divergence in the fact that Casey and co-workers assumed a symmetric reaction coordinate, which is not supported by QM calculations.[12−16] The transition states should not be interpolated linearly between idealized trigonal bipyramidal and quadratic planar geometries, respectively, for this interpolation is in strong contradiction to the early nature of the model system transition states. Consequently, then, purely hypothetical geometries were used, thereby manipulating not only electronic but also steric influences. Based on calculations with such severe approximations, neither steric nor electronic reasons can be quoted for the differing regioselectivities of DIPHOS **4** and BISBI **5**. Based on calculations with our method, steric effects seem to be the main contributors, which is diametrical to the previous interpretation.[7] Quite apart from that,

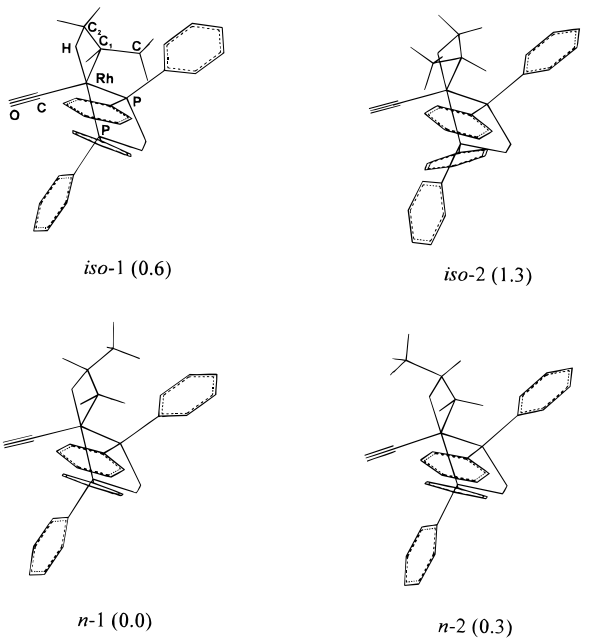

Figure 2. Calculated transition-state geometries for DIPHOS **4** (substrate = propene). Hydrogen atoms of the ligand are omitted for clarity; relative energies $E^{\#}$ (kcal·mol^{-1}) are given in parentheses.

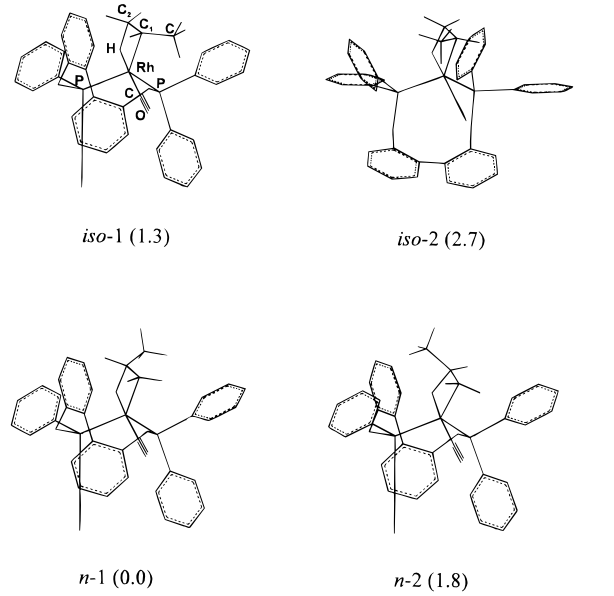

Figure 3. Calculated transition-state geometries for BISBI **5** (substrate = propene). Hydrogen atoms of the ligand are omitted for clarity, relative energies $E^{\#}$ (kcal·mol^{-1}) are given in parentheses.

(33) Gleich, D.; Schmid, R.; Herrmann, W. A. *Organometallics* **1998**, *17*, 2141.

(34) For the calculation of regioselectivities, Casey and co-workers used only the *iso*- or *n*-transition state that was lower in energy. On the contrary, we used both *iso*- and *n*-transition states (see text).

Table 9. Ligand Regioselectivities $S_{n/iso}$ of Additional Coordination Modes (Substrate = Propene)

ligand	coordination mode[a]	$S_{n/iso}$ (calc)
TPP	ee	3.5:1
	ae	41.0:1
	e[b]	2.0:1
	a[c]	9.6:1
BISBI	ae-1	59.8:1
	ae-2	43.5:1
NAPHOS	ae-1	41.3:1
	ae-2	29.2:1

[a] Cf. Scheme 3. [b] e = one TPP ligand, equatorially coordinated. [c] a = one TPP ligand, axially coordinated.

a correction of *iso*- and *n*-transition-state energies has not been mentioned in the paper, and it also remains open if the global minima have been searched for by MD simulations.

Finally, we want to point out further aspects. Unlike DIPHOS **4**, BISBI **5** (and analogously NAPHOS **6**) are flexible ligands. This can be seen from Figures 2 and 3: Whereas the geometry of the DIPHOS five-membered ring hardly varies within all four transition states, the nine-membered ring of BISBI switches between two quite dissimilar conformations. For both ligands, the transition states of highest and lowest energy, respectively, are *iso-2* and *n-1*. For BISBI, *iso-2* lies more than 1 kcal·mol^{-1} above *iso-2* of DIPHOS and accounts for the higher regioselectivity, though *n-2*/BISBI is far more shifted in energy than *n-2*/DIPHOS. It is interesting to estimate the role of the ligand backbone: For both ligands, the phenyl groups mainly cause the spacing between *iso-2* and *n-1*, and the backbone acts indirectly (note the backbone arrangement in the case of *iso-2*/BISBI and the distortion of axial phenyl groups in the case of *iso-2*/DIPHOS), whereas the shifting of *n-2*/BISBI is mainly dictated by the backbone. Except of *iso-2*, the backbone arrangements of BISBI are very similar. The flexibility of BISBI/NAPHOS has also been demonstrated by MD simulations,[22] but is not considered by the bite angle concept.[10] Therefore, we have taken into account an axial−equatorial arrangement, too. Owing to the axial chirality of these ligands, two distinct coordination modes ae-1 and ae-2 are possible (cf. Scheme 3). The corresponding *n*:*iso* ratios are listed in Table 9; they are much higher than for the equatorial−equatorial coordination mode, a result repugnant not to experimental results but to NBA correlations.[10,11] The selectivity ranking of BISBI **5** and NAPHOS **6** is now reversed: $S_{\mathrm{NAPHOS}} < S_{\mathrm{BISBI}}$. It should be noted that all axially−equatorially coordinated transition states are about 7 kcal/mol higher in total energy than corresponding bisequatorially coordinated transition states. The contribution of these axial−equatorial coordination modes to the experimentally observed regioselectivities is under current investigation. For estimating the regioselectivities of TPP, more than one coordination mode has to be considered (Table 9). Coordination of two TPP ligands leads to a higher regioselectivity than equatorial arrangement of one TPP ligand. Axial arrangement of one TPP ligand raises the *n*:*iso* ratio over that of equatorially−equatorially coordinated ligands. The latter result is not in accord with the qualitative treatment mentioned in the Introduction. However, it must be kept in mind to what extent electronic effects regulate the distribution of one TPP ligand in *trans*- or *cis*-position to the hydrido ligand. Axial arrangement of one PH_3 ligand has proven to be clearly unfavored in square-planar rhodium complexes preceding olefin coordination and insertion.[16]

Concluding Remarks

Hydroformylation regioselectivites of "real" rhodium−phosphine catalyst systems are accessible through a perspicuous formula and MM calculations with frozen reaction centers which have been obtained by QM calculations on model systems. The fundamental difference in regioselectivities between aliphatic and conjugated olefins, however, is not reproduced since, in the latter case, strong electronic effects are dominant which cannot be described by MM methods. Owing to several assumptions of the model and difficulties of the parametrization process, only relative estimates can be expected. On the other hand, a more sophisticated treatment via coupled QM/MM optimizations[16,19] is semiquantitative, too. Besides, the calculations are much more time-consuming: Apart from purely computational costs, small electronic influences produce a similar variety of transition states as in the case of QM model systems. Our method is also useful for the explanation of hydroformylation stereoselectivities,[33] the more so as the "substrate problem" then is of minor importance.

Acknowledgment. This work was generously supported by the Deutsche Forschungsgemeinschaft and the Fonds der Chemischen Industrie. We thank the Leibniz Rechenzentrum München for excellent service as well as R. Eckl and F. Rampf for various helpful discussions.

Supporting Information Available: A list of force field parameters, force field potentials, and coordinates of several structures (8 pages). See any current masthead page for ordering and Internet access instructions.

OM980459Q